


Article

# Synthesis and Electroluminescence Properties of 3-(Trifluoromethyl)phenyl-Substituted 9,10-Diarylanthracene Derivatives for Blue Organic Light-Emitting Diodes

Sang Woo Kwak <sup>1,†</sup>, Kang Mun Lee <sup>2,†</sup>, Ji-Eun Lee <sup>1</sup>, Jisu Yoo <sup>3</sup>, Yeonjin Yi <sup>3</sup>, Hyoshik Kwon <sup>4</sup>, Hyunbok Lee <sup>5,\*</sup>, Myung Hwan Park <sup>4,\*</sup>  and Yongseog Chung <sup>1,\*</sup>

<sup>1</sup> Department of Chemistry, Chungbuk National University, Cheongju 28644, Korea; sangwoo814@hanmail.net (S.W.K.); 01064342274@hanmail.net (J.-E.L.)

<sup>2</sup> Department of Chemistry, Institute for Molecular Science and Fusion Technology, Kangwon National University, Chuncheon 24341, Korea; kangmunlee@kangwon.ac.kr

<sup>3</sup> Institute of Physics and Applied Physics, Yonsei University, Seoul 03722, Korea; gotsson@naver.com (J.Y.); yeonjin@yonsei.ac.kr (Y.Y.)

<sup>4</sup> Department of Chemistry Education, Chungbuk National University, Cheongju 28644, Korea; hskwon@chungbuk.ac.kr

<sup>5</sup> Department of Physics, Kangwon National University, Chuncheon 24341, Korea

\* Correspondence: hyunbok@kangwon.ac.kr (H.L.); mhpark98@chungbuk.ac.kr (M.H.P.); yschung@chungbuk.ac.kr (Y.C.); Tel.: +82-33-250-8476 (H.L.); +82-43-261-2736 (M.H.P.); +82-43-261-2338 (Y.C.)

† These authors contributed equally to this work.

Received: 28 September 2017; Accepted: 23 October 2017; Published: 26 October 2017

**Abstract:** Diaryl-substituted anthracene derivatives containing 3-(trifluoromethyl)phenyl groups, 9,10-diphenyl-2-(3-(trifluoromethyl)phenyl)anthracene (**1**), 9,10-di([1,1'-biphenyl]-4-yl)-2-(3-(trifluoromethyl)phenyl)anthracene (**2**), and 9,10-di(naphthalen-2-yl)-2-(3-(trifluoromethyl)phenyl)anthracene (**3**) were synthesized and characterized. The compounds **1–3** possessed high thermal stability and proper frontier-energy levels, which make them suitable as host materials for blue organic light-emitting diodes. The electroluminescent (EL) emission maximum of the three *N,N*-diphenylamino phenyl vinyl biphenyl (DPAVBi)-doped (8 wt %) devices for compounds **1–3** was exhibited at 488 nm (for **1**) and 512 nm (for **2** and **3**). Among them, the **1**-based device displayed the highest device performances in terms of brightness ( $L_{\max} = 2153.5 \text{ cd}\cdot\text{m}^{-2}$ ), current efficiency ( $2.1 \text{ cd}\cdot\text{A}^{-1}$ ), and external quantum efficiency (0.8%), compared to the **2**- and **3**-based devices.

**Keywords:** anthracene; organic light-emitting diodes (OLED); blue-host material; electroluminescence

## 1. Introduction

Since the first report of Tang and VanSlyke in 1987 [1], organic electroluminescent (EL) devices have been receiving much scientific and commercial attention because of their latent capabilities, such as full-color displays, excellent brightness, fast response time, low turn-on voltage, wide viewing angle, and flexible light source [2]. Extremely pure red, green, and blue luminophores with high electrochemical stability and efficiency are particularly essential for a vivid full-color display in organic light-emitting diodes (OLEDs). To date, OLED materials for red and green emission with high performance have been developed [3–11]. However, continuous efforts to enhance stability and efficiency in blue fluorescent materials, which possess relatively low chemical and electrochemical properties, caused by the intrinsic wide band-gap, are still required [12,13].

As a notable candidate for effective blue-emitting materials, anthracene derivatives have attracted much attention in OLEDs because of their excellent optical and electroluminescent properties [14–28]. However, these organic fluorescent  $\pi$ -conjugated compounds pose small problems, such as poor thermal stability and device failure caused by intermolecular  $\pi$ -stacking features. Novel silicon-cored (triphenylsilane) [29,30] or asymmetric anthracene derivatives [31–33] containing bulky aryl substituents at the 9,10-position that exhibit high thermal stability and good EL properties as blue host materials have recently been investigated. Furthermore, 9,10-diarylanthracene (DAA) compounds containing aryl groups such as spirobifluorene [34] and carbazole [35,36] moieties are advantageous in terms of preventing close packing of the molecular structure, thereby achieving high quantum efficiency and EL properties. Along with the foregoing studies, DAA derivatives bearing various substituents at the C-2 position of anthracene moieties have also been recently investigated [37,38].

In an effort to extend such concepts, we were interested in the DAA compounds with trifluoromethyl units at the C-2 position of the anthracene core. The trifluoromethyl group, in particular, can give rise to enhancing electron mobility, thereby improving the balance of charge injection and transfer [39]. In addition, the introduction of a bulky 3-(trifluoromethyl)phenyl unit into the anthracene core can efficiently prevent the intermolecular aggregations and reduce self-quenching behaviors. Although several fluorinated DAA derivatives at the 9,10-position of the anthracene groups as noticeable blue host materials have been reported [40,41], the example of 2-fluorinated DAA compounds has never been studied.

From this perspective, we have systematically designed and synthesized a series of DAA derivatives (i.e., 9,10-diphenyl-2-(3-(trifluoromethyl)phenyl)anthracene (**1**), 9,10-di([1,1'-biphenyl]-4-yl)-2-(3-(trifluoromethyl)phenyl)anthracene (**2**), and 9,10-di(naphthalen-2-yl)-2-(3-(trifluoromethyl)phenyl)anthracene (**3**)) bearing fluorinated end-capping groups at the C-2 position of the anthracene core to investigate their thermal/electrochemical stabilities and electronic performances. The synthesis, characterization, and luminescence properties of the newly prepared DAA compounds (**1–3**), along with their application as the blue host materials for OLEDs, are presented in detail herein.

## 2. Materials and Methods

### 2.1. General Considerations

All chemicals were purchased from Sigma-Aldrich (St. Louis, MO, USA) and were used without any further purification. All solvents, such as toluene, tetrahydrofuran (THF), and ethanol, were dried by distillation from sodium diphenylketyl under dinitrogen and were stored over 5 Å activated molecular sieves [42]. Spectrophotometric-grade dichloromethane (DCM) was used as received. All reactions were carried out under a nitrogen atmosphere. Commercial reagents were used without any further purification after purchasing from Sigma-Aldrich (bromobenzene, 4-bromobiphenyl, 2-bromonaphthalene, *n*-butyllithium solution (2.5 M in hexane, *n*-BuLi), potassium iodide (KI), sodium hypophosphite (NaPO<sub>2</sub>H<sub>2</sub>), acetic acid, 3-trifluoromethylphenylboronic acid, copper iodide (CuI), tetrakis(triphenylphosphine)palladium (Pd(PPh<sub>3</sub>)<sub>4</sub>), potassium carbonate (K<sub>2</sub>CO<sub>3</sub>). The 2-bromo-9,10-arylanthracene precursors (**1a–3a**) were analogously prepared according to the reported procedures [38,43]. Deuterated solvent (CDCl<sub>3</sub>) from Cambridge Isotope Laboratories (Tewksbury, MA, USA) was used after drying over activated molecular sieves (5 Å). Nuclear Magnetic Resonance (NMR) spectra were recorded at ambient temperature on Bruker Avance 400 spectrometer (400.13 MHz for <sup>1</sup>H, 100.62 MHz for <sup>13</sup>C, and 376.5 MHz for <sup>19</sup>F) using standard parameters. Chemical shifts are given in ppm, and are referenced against external Me<sub>4</sub>Si (<sup>1</sup>H, <sup>13</sup>C) and CFCl<sub>3</sub> (<sup>19</sup>F). Elemental analyses were performed on an EA3000 (Eurovector, Pavia, Italy) in the Central Laboratory of Kangwon National University. The thermal properties of compound were investigated by TGA2940 system (TA Instrument, New Castle, DE, USA) and DSC2910 system (TA Instrument, New Castle, DE, USA) under a nitrogen atmosphere at a heating rate of 10 °C/min.

UV/Vis absorption and PL spectra were recorded on a Jasco V-530 (Jasco, Easton, MD, USA) and a Spex Fluorog-3 Luminescence spectrophotometer (HORIBA, Edison, NJ, USA), respectively, in CH<sub>2</sub>Cl<sub>2</sub> solvent with a 1-cm quartz cuvette at ambient temperature. Cyclic voltammetry measurements were performed using an AUTOLAB/PGSTAT12 system (Artisan Technology Group, Champaign, IL, USA).

## 2.2. General Synthesis of 9,10-aryl-2-(3-(trifluoromethyl)phenyl)anthracene (1–3)

The mixture of the relevant 2-bromo-9,10-arylanthracene precursor (1.00 mmol), 3-trifluoromethylphenylboronic acid (0.30 g, 1.58 mmol), Pd(PPh<sub>3</sub>)<sub>4</sub> (0.06 g, 0.05 mmol) and K<sub>2</sub>CO<sub>3</sub> (0.76 g, 5.50 mmol) was added to the solvent of 24 mL (toluene/H<sub>2</sub>O/ethanol = 2:1:1, *v/v/v*) at ambient temperature. After stirring for 1 h, the reaction mixture was allowed to slowly heated to 110 °C and stirred for 24 h. The resulting solution was extracted with CH<sub>2</sub>Cl<sub>2</sub> (30 mL × 3). The combined organic portions were dried over MgSO<sub>4</sub> and the solvent was removed under reduced pressure. Purification by column chromatography (eluent: ethylacetate/*n*-hexane = 1:10, *v/v*) afforded the products (1–3).

### 2.2.1. Data for 9,10-diphenyl-2-(3-(trifluoromethyl)phenyl)anthracene (1)

Pale yellow solid (0.24 g, 48%). <sup>1</sup>H NMR (CDCl<sub>3</sub>): δ 7.89 (d, *J* = 1.2 Hz, 1H), 7.80 (d, *J* = 8.2 Hz, 1H), 7.77 (br s, 1H), 7.72 (d, *J* = 7.2 Hz, 1H), 7.70 (d, *J* = 4.8 Hz, 1H), 7.68 (d, *J* = 7.8 Hz, 1H), 7.61 (m, 4H), 7.56 (m, 4H), 7.51 (m, 5H), 7.34 (q, *J* = 8.0 Hz, 2H). <sup>13</sup>C NMR (CDCl<sub>3</sub>): δ 141.92, 138.80, 138.66, 137.73, 137.14, 135.85, 131.29, 131.27, 130.96, 130.55, 130.39, 130.22, 129.84, 129.25, 129.13, 128.53, 128.49, 128.08, 127.71, 127.62, 127.03, 127.01, 125.45, 125.33, 125.31, 125.05, 124.48, 124.05, 124.01, 123.92, 123.88, 122.75, 77.20 (CF<sub>3</sub>). <sup>19</sup>F NMR (CDCl<sub>3</sub>): δ−62.7. Anal. Calcd. for C<sub>33</sub>H<sub>21</sub>F<sub>3</sub>: C, 83.53; H, 4.46. Found: C, 82.99; H, 4.13.

### 2.2.2. Data for 9,10-di([1,1'-biphenyl]-4-yl)-2-(3-(trifluoromethyl)phenyl)anthracene (2)

Pale yellow solid (0.30 g, 44%). <sup>1</sup>H NMR (CDCl<sub>3</sub>): δ 7.99 (d, *J* = 1.2 Hz, 1H), 7.91 (d, *J* = 8.0 Hz, 1H), 7.86 (d, *J* = 7.6 Hz, 4H), 7.84 (m, 1H), 7.80 (m, 4H), 7.78 (d, *J* = 1.2 Hz, 2H), 7.71 (d, *J* = 8.0 Hz, 1H), 7.61 (m, 4H), 7.58 (m, 1H), 7.52 (m, 6H), 7.42 (m, 2H), 7.39 (m, 2H). <sup>13</sup>C NMR (CDCl<sub>3</sub>): δ 141.92, 140.78, 140.74, 140.44, 137.77, 137.65, 137.43, 136.89, 136.03, 131.79, 131.75, 131.29, 130.97, 130.62, 130.49, 130.31, 129.91, 129.29, 129.22, 128.93, 128.15, 127.51, 127.21, 127.19, 127.16, 127.09, 127.07, 125.46, 125.44, 125.06, 124.63, 124.10, 124.06, 123.96, 123.92, 122.75, 77.20 (CF<sub>3</sub>). <sup>19</sup>F NMR (CDCl<sub>3</sub>): δ−62.6. Anal. Calcd. for C<sub>45</sub>H<sub>29</sub>F<sub>3</sub>: C, 86.24; H, 4.66. Found: C, 85.78; H, 4.20.

### 2.2.3. Data for 9,10-di(naphthalen-2-yl)-2-(3-(trifluoromethyl)phenyl)anthracene (3)

Pale yellow solid (0.31 g, 46%). <sup>1</sup>H NMR (CDCl<sub>3</sub>): δ 8.11 (d, *J* = 7.78 Hz, 2H), 8.04 (m, 4H), 7.94 (m, 3H), 7.86 (d, *J* = 8.0 Hz, 1H), 7.74 (m, 3H), 7.66 (m, 3H), 7.61 (m, 4H), 7.54 (dd, *J* = 8.2, 7.6 Hz, 1H), 7.50 (d, *J* = 7.6 Hz, 1H), 7.42 (t, *J* = 8.4 Hz, 2H), 7.32 (q, *J* = 8.2 Hz, 2H). <sup>13</sup>C NMR (CDCl<sub>3</sub>): δ 141.84, 137.62, 137.12, 136.31, 136.21, 136.17, 133.44, 133.42, 132.86, 132.82, 131.20, 130.88, 130.65, 130.42, 130.33, 130.25, 130.00, 129.47, 129.45, 129.33, 129.24, 128.20, 128.16, 128.15, 128.11, 127.96, 127.94, 127.14, 127.10, 126.54, 126.50, 126.33, 125.48, 125.44, 125.09, 124.73, 124.08, 124.04, 123.93, 122.70, 77.20 (CF<sub>3</sub>). <sup>19</sup>F NMR (CDCl<sub>3</sub>): δ−62.6. Anal. Calcd. for C<sub>41</sub>H<sub>25</sub>F<sub>3</sub>: C, 85.70; H, 4.39. Found: C, 85.21; H, 3.98.

## 2.3. Cyclic Voltammetry

Cyclic voltammetry measurements of 1–3 were performed by a three-electrode cell configuration system consisting of platinum working and counter electrodes and a Ag/AgNO<sub>3</sub> (0.1 M in CH<sub>3</sub>CN) reference electrode at room temperature. The solvent was acetonitrile (CH<sub>3</sub>CN) and 0.1 M tetrabutylammonium hexafluorophosphate was used as the supporting electrolyte. All solvents were sufficiently degassed for 1 h before use. The oxidation potentials were recorded at a scan rate of 100 mV/s and reported with reference to the ferrocene/ferrocenium (Fc/Fc<sup>+</sup>) redox couple.

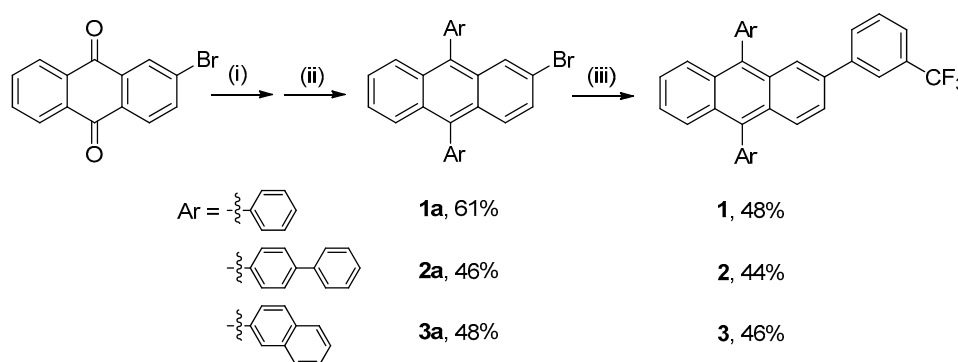
## 2.4. Device Fabrication and Characterization

The OLED devices were fabricated on glass substrates precoated with a 150 nm thick indium tin oxide (ITO) layer with a sheet resistance of  $\sim 10 \Omega$  per square. The ITO glass was cleaned with ultrasonication in deionized (DI) water, detergent, acetone, methanol and DI water for 10 min each in sequence. Then, the ITO substrate was dried with  $N_2$  gas flow and treated with UV-ozone for 15 min at  $100^\circ C$ . After the cleaning procedure, the ITO substrate was loaded into a high-vacuum chamber at a base pressure of  $<1.0 \times 10^{-7}$  Torr. The 4,4'-bis[*N*-(1-naphthyl)-*N*-phenylamino]biphenyl (NPB), tris(8-hydroxyquinolino)aluminum ( $Alq_3$ ), and DPAVBi were purchased from Luminescence Technology Corp. and they were used without further purification. The organic materials and LiF were sequentially deposited onto the substrate with thermal evaporation using Knudsen cells. The NPB and  $Alq_3$  were deposited with a rate of  $0.8 \text{ \AA}\cdot\text{s}^{-1}$  while each host material and DPAVBi were codeposited with a rate of  $0.2 \text{ \AA}\cdot\text{s}^{-1}$  and  $0.016 \text{ \AA}\cdot\text{s}^{-1}$ . After that, the sample was transferred to another high-vacuum chamber without breaking vacuum, and then Al was deposited using a BN boat at a rate of  $\sim 1 \text{ \AA}\cdot\text{s}^{-1}$ . The total thicknesses and deposition rates were monitored with a quartz crystal microbalance. The device area was  $0.04 \text{ cm}^2$ . The current density–voltage–luminance ( $J$ – $V$ – $L$ ) characteristics of the OLEDs were measured using two Keithley 2400 source measure units and a Si photodiode. The electroluminescence (EL) spectra were measured using a PR650 spectroradiometer (StellarNet Inc., Tampa, FL, USA). Assuming Lambertian emission, the external quantum efficiency (EQE) was calculated from the measured  $J$ – $V$ – $L$  characteristics and EL spectrum.

## 3. Results and Discussion

### 3.1. Synthesis and Characterization

Scheme 1 shows the synthetic routes for new 3- $CF_3$ -phenyl substituted DAA compounds 1–3. The precursors (1a–3a) of the anthracene derivatives were produced by the reaction between 2-bromoanthracene-9,10-dione and lithium salts of each bromoaryl compound, followed by acidification in a relatively high yield (i.e., 46–61%). These precursors could be readily converted into the final products 1–3 from the Suzuki–Miyaura coupling with (3- $CF_3$ -phenyl) boronic acid in moderate yields (44–48%). The formation of compounds 1–3 was confirmed by  $^1H$ ,  $^{13}C$  NMR,  $^{19}F$  NMR spectroscopy (Figures S1–S6, Supplementary Materials), and elemental analysis (EA). The  $^1H$  and  $^{13}C$  NMR spectra of all DAA derivatives were in good agreement with the predicted structures. The  $^{19}F$  NMR signals of 1–3 detected around  $\delta$ –62 ppm also indicated the presence of the  $CF_3$ -phenyl unit. Moreover, the chemical shifts of the resonances associated with the proton and carbon atoms in these molecules were in the expected range.



**Scheme 1.** Synthetic routes for diarylanthracene (DAA) derivatives 1–3. Reagents and conditions: (i) bromobenzene (for 1), 4-bromobiphenyl (for 2) or 2-bromonaphthalene (for 3), *n*-BuLi, THF,  $-78^\circ C$ , (ii) KI,  $NaPO_2H_2$ , acetic acid, (iii) 3-trifluoromethylphenylboronic acid, CuI,  $Pd(PPh_3)_4$ ,  $K_2CO_3$ , toluene/ $H_2O$ /ethanol (*v/v/v*, 2:1:1),  $110^\circ C$ , 24 h.

### 3.2. Thermal Properties

The thermal properties of DAA derivatives **1–3** were examined by thermogravimetric analysis (TGA) and differential scanning calorimetry (DSC) under dinitrogen atmosphere. Compounds **1–3** exhibited  $T_{d5}$  values of 262, 387, and 358 °C, respectively, indicating that the terminal naphthyl and biphenyl groups showed greater heat-resistant properties than the phenyl moiety. Such a good thermal stability of compounds **1–3** was enough to stand the high temperature for the vacuum vapor deposition. These results clearly showed that the bulky aromatic groups on the C9 and C10 positions of the anthracene moiety led to an enhanced thermal stability. A DSC analysis was performed from 25 to 125 °C (for **1**) or 180 °C (for **2** and **3**) at a heating rate of 10 °C/min to investigate the morphological stability of **1–3**. Figure 1 shows that the glass transition temperature ( $T_g$ ) of **1–3** was obtained at 65, 121, and 118 °C, respectively.

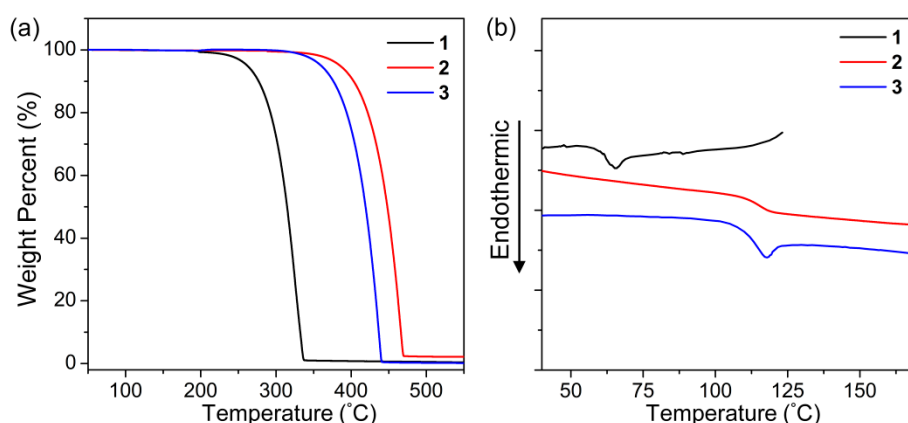


**Figure 1.** (a) Thermogravimetric Analysis (TGA) curves and (b) the second heating differential scanning calorimetry (DSC) curves of **1–3** at 10 °C/min.

### 3.3. Photophysical and Electrochemical Properties

The photophysical properties of DAA compounds **1–3** were investigated by UV–Vis absorption and photoluminescence (PL) spectroscopy (Figure 2 and Table 1). The absorption spectra of **1–3** in dichloromethane ( $1.0 \times 10^{-5}$  M) displayed the typical  $\pi\pi^*$  vibronic transition patterns ( $\lambda_{\text{abs}} = 365$ , 384, and 405 nm for **1** and  $\lambda_{\text{abs}} = 367$ , 386, and 407 nm for **2** and **3**, Table 1) derived from the isolated anthracene moieties. The absorption maximum point ( $\lambda_{\text{abs}}$ ) of **2** and **3** was slightly red-shifted by ca. 2 nm compared to that of compound **1**. These features were also shown in the fluorescence spectra of each compound. The emission maxima ( $\lambda_{\text{em}}$ ) of **1–3** were observed at 429 nm for **1** and 439 nm for **2** and **3** (Table 1), respectively. Accordingly, the red-shifted spectra of **2** and **3** distinctively implied that both the naphthyl and biphenyl moiety had a slightly stronger electron-donating property than the phenyl group and, thus, could induce the narrow band gaps. The band gaps estimated from the absorption edge for **2** and **3** were indeed slightly narrower than that of **1** (2.93 eV for **2** or **3** and 2.98 eV for **1**, Table 1). Furthermore, the PL spectra of all compounds were similar to the previously reported DAA derivatives (Figure 2) [44] assignable to the lowest  $\pi\pi^*$  transition on the anthracene units.

The electrochemical properties of **1–3** were examined by cyclic voltammetry (CV) measurements (Figure 3). From the first oxidation onset potential, the highest occupied molecular orbital (HOMO) energy levels of **1–3** were calculated to be  $-5.51$ ,  $-5.61$ , and  $-5.55$  eV, respectively. The LUMO levels can be estimated by combining the HOMO level and the optical band gap ( $E_g$ ) determined from the edge of the UV–Vis absorption spectra. Consequently, the energy levels of **1–3** were also calculated as  $-2.53$ ,  $-2.69$ , and  $-2.62$  eV, respectively (Table 1). Such values indicated that DAA compounds **1–3** had suitable frontier energy levels and wide energy band gaps ( $E_g$ ) of ca. 2.9–3.0 eV as host materials

for blue emission in OLED. The quantum yields ( $\Phi$ ) of 1–3 were calculated as 0.24, 0.21 and 0.22, respectively, which are similar to each other (Table 1).

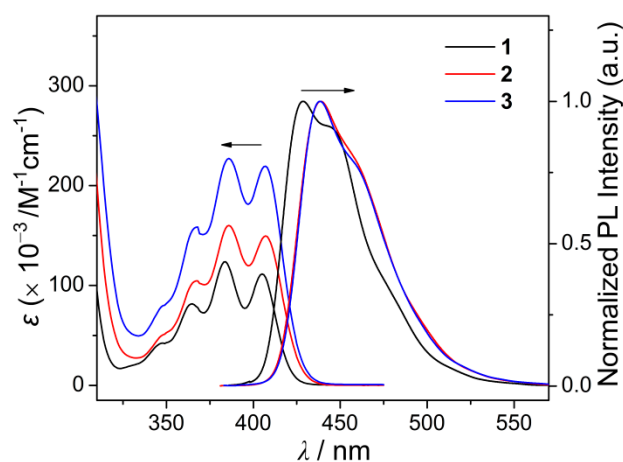


**Figure 2.** Ultraviolet-Visible (UV-Vis) absorption (left side) and photoluminescence (PL) spectra (right side) in dichloromethane ( $1.0 \times 10^{-5}$  M,  $\lambda_{\text{ex}} = 373$  nm) for 1–3.

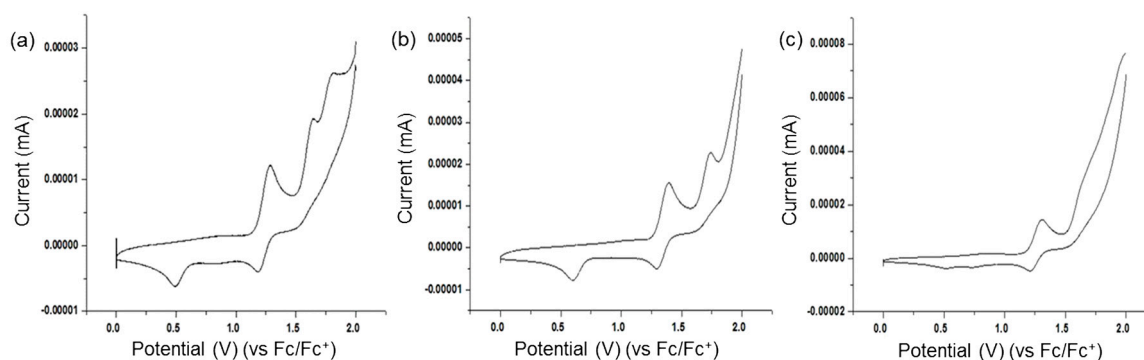


**Figure 3.** Cyclic voltammograms of (a) 1, (b) 2 and (c) 3 ( $5 \times 10^{-4}$  M in acetonitrile, scan rate = 100 mV/s).

**Table 1.** Photophysical and electrochemical properties of 1–3.

| Compound | $\lambda_{\text{abs}}^1$ (nm) | $\lambda_{\text{em}}^1$ (nm) | $E_g^2$ (eV) | $E_{\text{ox}}^3$ (V) | HOMO <sup>4</sup> (eV) | LUMO <sup>5</sup> (eV) | $T_g$ (°C) | $T_{d5}$ (°C) | $\Phi^6$ |
|----------|-------------------------------|------------------------------|--------------|-----------------------|------------------------|------------------------|------------|---------------|----------|
| 1        | 365, 384, 405                 | 429                          | 2.98         | 1.11                  | −5.51                  | −2.53                  | 65         | 262           | 0.24     |
| 2        | 367, 386, 407                 | 439                          | 2.93         | 1.22                  | −5.62                  | −2.69                  | 121        | 387           | 0.21     |
| 3        | 367, 386, 407                 | 439                          | 2.93         | 1.15                  | −5.55                  | −2.62                  | 118        | 358           | 0.22     |

<sup>1</sup>  $1.0 \times 10^{-5}$  M in  $\text{CH}_2\text{Cl}_2$ . <sup>2</sup> Estimated from the absorption edge. <sup>3</sup> Oxidation onset potential vs. a  $\text{Fc}/\text{Fc}^+$  couple.

<sup>4</sup> Calculated from the  $E_{\text{ox}}$ . <sup>5</sup> Estimated from the HOMO and band-gap ( $E_g$ ) energies. <sup>6</sup> Quantum yield measured using quinine sulfate as a standard (0.5 M  $\text{H}_2\text{SO}_4$ ,  $r\Phi = 0.55$ ) in  $\text{CH}_2\text{Cl}_2$  ( $1.0 \times 10^{-5}$  M). HOMO, highest occupied molecular orbital; LUMO, lowest unoccupied molecular orbital.

### 3.4. Electroluminescent Properties

The anthracene-based compounds 1–3 were investigated as blue host materials by fabricating multi-layer OLEDs with a DPAVBi dopant. Figure 4 presents the energy diagram of the OLEDs and the molecular structure of the organic materials used in the OLEDs. NPB was selected as the hole transport layer (HTL) material due to its having similar HOMO energy levels to 1–3 (ca. 5.5–5.6 eV) and NPB (ca. 5.4 eV). Figure 4 illustrates that the devices were fabricated with the following configuration:

ITO/NPB (40 nm)/**1**, **2**, or **3** (30 nm, DPAVB<sub>i</sub> (8 wt %))/Alq<sub>3</sub> (30 nm)/LiF (0.5 nm)/Al (100 nm) device, where ITO is the anode; NPB is the HTL; the chemically purified anthracene derivatives **1**, **2** or **3** (host) and DPAVB<sub>i</sub> (dopant) served as the emission layer (EML); Alq<sub>3</sub> was the electron transport layer (ETL); and a thin LiF served as the electron injection layer at the Al cathode interface.

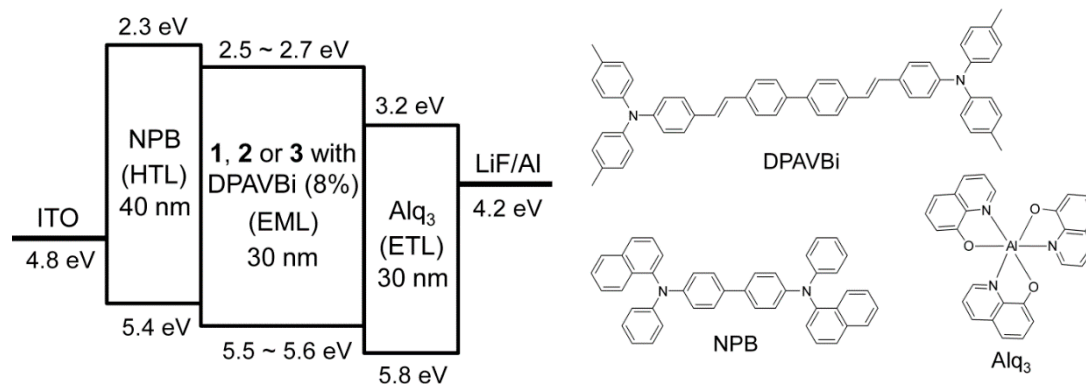


**Figure 4.** Energy diagram of the organic light-emitting diodes (OLEDs) using **1–3** with *N,N*-diphenylamino phenyl vinyl biphenyl (DPAVB<sub>i</sub>) (8 wt %) as an emitter and molecular structures of each compound; NPB, 4,4'-bis[*N*-(1-naphthyl)-*N*-phenylamino]biphenyl; ITO, indium tin oxide; HTL, hole transport layer; EML, ETL, emission layer; electron transport layer.

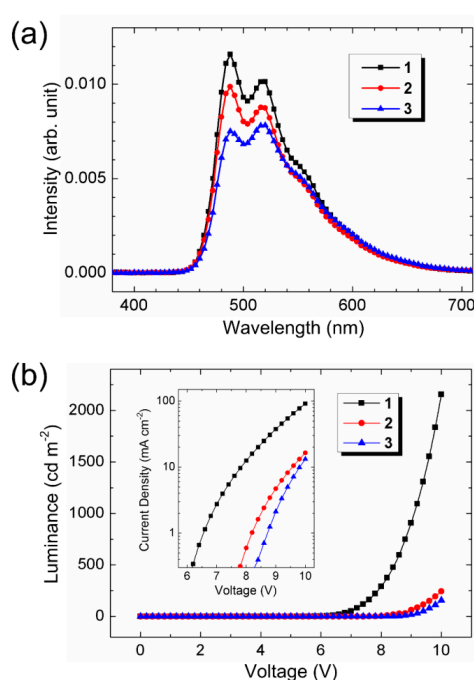
Figure 5a shows the EL spectra of the OLEDs using **1–3** with a DPAVB<sub>i</sub> dopant. All devices exhibited the expected blue emissions and their main EL peaks were commonly observed at 488 and 512 nm with a shoulder peak at 556 nm. The peak intensity at 512 nm was somewhat higher than the reported EL features of DPAVB<sub>i</sub>, which was attributed to the slight emission from Alq<sub>3</sub>. The maximum EL peak was observed at 488 nm for **1** and **2** and at 512 nm for **3** because of the increased Alq<sub>3</sub> emission originating from the inefficient charge transport to the EML in **3**-based OLEDs.

Figure 5b shows the measured *L–V* characteristics of the **1–3**-based OLEDs with an 8 wt % ratio of DPAVB<sub>i</sub>. At 10 V, the **1–3**-based OLEDs showed an *L* of 2153.5, 243.0, and 156.3 cd·m<sup>−2</sup>, respectively. The inset shows the measured *J–V* characteristics of the OLEDs. Moreover, at 10 V, the **1–3**-based OLEDs presented a *J* of 91.6, 16.4, and 13.2 mA·cm<sup>−2</sup>, respectively. We defined the turn-on and operating voltages as the voltages providing the *L* of 1 and 100 cd·m<sup>−2</sup>. As a result, the turn-on voltage of the **1–3**-based OLEDs was 6.0, 7.8, and 8.5 V, while the operating voltage was 7.4, 9.4, and 9.8 V, respectively. The current efficiency of **1–3** based OLEDs at the operating voltage was 2.1, 1.4, and 1.1 cd A<sup>−1</sup>, respectively. Meanwhile, the power efficiency of the **1–3**-based OLEDs at the operating voltage was 0.9, 0.5, and 0.4 lm·W<sup>−1</sup>. Combining the *J–V–L* characteristics and the EL spectra, the external quantum efficiency (EQE) of the **1–3**-based OLEDs at the operating voltage was calculated as 0.8%, 0.5%, and 0.4%. The Commission Internationale de l’Eclairage (CIE) color coordinates for **1–3** appeared at (0.25, 0.51), (0.25, 0.51), and (0.27, 0.52), respectively. Table 2 summarizes the measured device parameters. These results clearly indicated that the **1**-based OLEDs showed superior charge transport and light emission abilities among all devices. Although the turn-on voltages of these devices were a little high, and the efficiencies was not outstanding, the results exhibit the possibilities of these anthracene-based compounds as blue-host materials in OLEDs.

**Table 2.** Device parameters of the 1–3-based organic light-emitting diodes (OLEDs) from the current density–voltage–luminance ( $J$ – $V$ – $L$ ) characteristics and the electroluminescent (EL) spectra.

| Compound | Turn-on Voltage <sup>1</sup> (V) | Operating Voltage <sup>2</sup> (V) | Current Efficiency <sup>3</sup> (cd·A <sup>−1</sup> ) | Power Efficiency <sup>3</sup> (lm·W <sup>−1</sup> ) | EQE <sup>3</sup> (%) | CIE (x, y)   |
|----------|----------------------------------|------------------------------------|---|---|----------------------|--------------|
| 1 (8%)   | 6.0                              | 7.4                                | 2.1   | 0.9   | 0.8                  | (0.25, 0.51) |
| 2 (8%)   | 7.8                              | 9.4                                | 1.4   | 0.5   | 0.5                  | (0.25, 0.51) |
| 3 (8%)   | 8.5                              | 9.8                                | 1.1   | 0.4   | 0.4                  | (0.27, 0.52) |

<sup>1</sup> Voltage at 1 cd/m<sup>2</sup>. <sup>2</sup> Voltage at 100 cd/m<sup>2</sup>. <sup>3</sup> Detected at the operating voltage. EQE, external quantum efficiency; CIE, Commission Internationale de l'Éclairage.

**Figure 5.** (a) EL spectra of the OLEDs using 1–3 with DPAVBi and (b)  $L$ – $V$  characteristics of the OLEDs (the inset shows  $J$ – $V$  characteristics).

#### 4. Conclusions

New anthracene-based blue-host materials 1–3 were synthesized and characterized in this study. The anthracene derivatives possessed high thermal stability and proper frontier-energy levels suitable as novel host materials for blue OLEDs. Relevant further studies using various anthracene derivatives to enhance the device performance are in progress.

**Supplementary Materials:** The following are available online at <http://www.mdpi.com/2076-3417/7/11/1109/s1>, Figures S1–S6 Multinuclear NMR spectra of compounds 1–3.

**Acknowledgments:** This work was supported by the Nano Material Technology Development Program (NRF-2016M3A7B4909246 for Kang Mun Lee) and Basic Science Research Program (NRF-2015R1C1A1A01055026 for Hyunbok Lee) through the National Research Foundation of Korea (NRF) funded by the Ministry of Science, ICT and Future Planning. Yongseog Chung acknowledges the Basic Science Research Program (NRF-2017R1D1A1B03031911) through the National Research Foundation of Korea (NRF) funded by the Ministry of Education and the support from the research grant of Chungbuk National University in 2015.

**Author Contributions:** Sang Woo Kwak and Ji-Eun Lee performed the experiments for synthesis of compounds and analyzed the data; Kang Mun Lee, Hyoshik Kwon, Myung Hwan Park and Yongseog Chung analyzed the



data and wrote the paper; Jisu Yoo, Yeonjin Yi and Hyunbok Lee performed the experiments for EL fabrications, analyzed the data and wrote the paper.

**Conflicts of Interest:** The authors declare no conflict of interest.

## References

1. Tang, C.W.; VanSlyke, S.A. Organic electroluminescent diodes. *Appl. Phys. Lett.* **1987**, *51*, 913–915. [[CrossRef](#)]
2. Burroughes, J.H.; Bradley, D.D.C.; Brown, A.R.; Marks, R.N.; Mackay, K.; Friend, R.H.; Burns, P.L.; Holmes, A.B. Light-emitting diodes based on conjugated polymers. *Nature* **1990**, *347*, 539–541. [[CrossRef](#)]
3. Kido, J.; Kimura, M.; Nagai, K. Multilayer white light-emitting organic electroluminescent device. *Science* **1995**, *267*, 1332–1334. [[CrossRef](#)] [[PubMed](#)]
4. D’Andrade, B.W.; Thompson, M.E.; Forrest, S.R. Controlling exciton diffusion in multilayer white phosphorescent organic light emitting devices. *Adv. Mater.* **2002**, *14*, 147–151. [[CrossRef](#)]
5. Li, J.; Zhang, T.; Liang, Y.; Yang, R. Solution-processible carbazole dendrimers as host materials for highly efficient phosphorescent organic light-emitting diodes. *Adv. Funct. Mater.* **2013**, *23*, 619–628. [[CrossRef](#)]
6. Lee, S.-J.; Park, J.-S.; Song, M.; Shin, I.A.; Kim, Y.-I.; Lee, J.W.; Kang, J.-W.; Gal, Y.-S.; Kang, S.; Lee, J.Y.; et al. Synthesis and characterization of red-emitting iridium(III) complexes for solution-processable phosphorescent organic light-emitting diodes. *Adv. Funct. Mater.* **2009**, *19*, 2205–2212. [[CrossRef](#)]
7. Thiery, S.; Tondelier, D.; Geffroy, B.; Jacques, E.; Robin, M.; Métivier, R.; Jeannin, O.; Rault-Berthelot, J.; Poriel, C. Spirobifluorene-2,7-dicarbazole-4'-phosphine oxide as host for high-performance single-layer green phosphorescent OLED devices. *Org. Lett.* **2015**, *17*, 4682–4685. [[CrossRef](#)] [[PubMed](#)]
8. Thiery, S.; Tondelier, D.; Declairieux, C.; Geffroy, B.; Jeannin, O.; Métivier, R.; Rault-Berthelot, J.; Poriel, C. 4-Pyridyl-9,9'-spirobifluorenes as host materials for green and sky-blue phosphorescent OLEDs. *J. Phys. Chem. C* **2015**, *119*, 5790–5805. [[CrossRef](#)]
9. Wang, Y.-K.; Sun, Q.; Wu, S.-F.; Yuan, Y.; Li, Q.; Jiang, Z.-Q.; Fung, M.-K.; Liao, L.-S. Thermally activated delayed fluorescence material as host with novel spiro-based skeleton for high power efficiency and low roll-off blue and white phosphorescent devices. *Adv. Funct. Mater.* **2016**, *26*, 7929–7936. [[CrossRef](#)]
10. Xue, M.-M.; Huang, C.-C.; Yuan, Y.; Cui, L.-S.; Li, Y.-X.; Wang, B.; Jiang, Z.-Q.; Fung, M.-K.; Liao, L.-S. De novo design of boron-based host materials for highly efficient blue and white phosphorescent OLEDs with low efficiency roll-off. *ACS Appl. Mater. Interfaces* **2016**, *8*, 20230–20236. [[CrossRef](#)] [[PubMed](#)]
11. Poriel, C.; Rault-Berthelot, J. Structure–property relationship of 4-substituted-spirobifluorenes as hosts for phosphorescent organic light emitting diodes: An overview. *J. Mater. Chem. C* **2017**, *5*, 3869–3897. [[CrossRef](#)]
12. Yang, X.; Xu, X.; Zhou, G. Recent advances of the emitters for high performance deep-blue organic light-emitting diodes. *J. Mater. Chem. C* **2015**, *3*, 913–944. [[CrossRef](#)]
13. Seifert, R.; Rabelo de Moraes, I.; Scholz, S.; Gather, M.C.; Lüssem, B.; Leo, K. Chemical degradation mechanisms of highly efficient blue phosphorescent emitters used for organic light emitting diodes. *Org. Electron.* **2013**, *14*, 115–123. [[CrossRef](#)]
14. Kim, D.Y.; Kim, Y.S.; Kim, S.H.; Jeong, S.; Lee, S.E.; Kim, Y.K.; Yoon, S.S. Synthesis and electroluminescent properties of *tert*-butylated arylamine substituted 9,10-diphenylanthracene derivatives for organic light-emitting diodes. *Synth. Met.* **2016**, *220*, 628–634. [[CrossRef](#)]
15. Wang, Z.; Liu, W.; Xu, C.; Ji, B.; Zheng, C.; Zhang, X. Excellent deep-blue emitting materials based on anthracene derivatives for non-doped organic light-emitting diodes. *Opt. Mater.* **2016**, *58*, 260–267. [[CrossRef](#)]
16. Park, J.K.; Lee, K.H.; Kang, S.; Lee, J.Y.; Park, J.S.; Seo, J.H.; Kim, Y.K.; Yoon, S.S. Highly efficient blue-emitting materials based on 10-naphthylanthracene derivatives for OLEDs. *Org. Electron.* **2010**, *11*, 905–915. [[CrossRef](#)]
17. Park, H.; Lee, J.; Kang, I.; Chu, H.Y.; Lee, J.-I.; Kwon, S.-K.; Kim, Y.-H. Highly rigid and twisted anthracene derivatives: A strategy for deep blue OLED materials with theoretical limit efficiency. *J. Mater. Chem.* **2012**, *22*, 2695–2700. [[CrossRef](#)]
18. Cho, I.; Kim, S.H.; Kim, J.H.; Park, S.; Park, S.Y. Highly efficient and stable deep-blue emitting anthracene-derived molecular glass for versatile types of non-doped OLED applications. *J. Mater. Chem.* **2012**, *22*, 123–129. [[CrossRef](#)]
19. Bin, J.-K.; Hong, J.-I. Efficient blue organic light-emitting diode using anthracene-derived emitters based on polycyclic aromatic hydrocarbons. *Org. Electron.* **2011**, *12*, 802–808. [[CrossRef](#)]

20. Lee, K.H.; You, J.N.; Kang, S.; Lee, J.Y.; Kwon, H.J.; Kim, Y.K.; Yoon, S.S. Synthesis and electroluminescent properties of blue-emitting *t*-butylated bis(diarylaminoaryl) anthracenes for OLEDs. *Thin Solid Films* **2010**, *518*, 6253–6258. [[CrossRef](#)]
21. Zheng, C.-J.; Zhao, W.-M.; Wang, Z.-Q.; Huang, D.; Ye, J.; Ou, X.-M.; Zhang, X.-H.; Lee, C.-S.; Lee, S.-T. Highly efficient non-doped deep-blue organic light-emitting diodes based on anthracene derivatives. *J. Mater. Chem.* **2010**, *20*, 1560–1566. [[CrossRef](#)]
22. Kim, S.-K.; Yang, B.; Ma, Y.; Lee, J.-H.; Park, J.-W. Exceedingly efficient deep-blue electroluminescence from new anthracenes obtained using rational molecular design. *J. Mater. Chem.* **2008**, *18*, 3376–3384. [[CrossRef](#)]
23. Park, J.-Y.; Jung, S.Y.; Lee, J.Y.; Baek, Y.G. High efficiency in blue organic light-emitting diodes using an anthracene-based emitting material. *Thin Solid Films* **2008**, *516*, 2917–2921. [[CrossRef](#)]
24. Shih, P.-I.; Chuang, C.-Y.; Chien, C.-H.; Diao, E.W.-G.; Shu, C.-F. Highly efficient non-doped blue-light-emitting diodes based on an anthracene derivative end-capped with tetraphenylethylene groups. *Adv. Funct. Mater.* **2007**, *17*, 3141–3146. [[CrossRef](#)]
25. Zhang, Y.; Lai, S.-L.; Tong, Q.-X.; Lo, M.-F.; Ng, T.-W.; Chan, M.-Y.; Wen, Z.-C.; He, J.; Jeff, K.-S.; Tang, X.-L.; et al. High efficiency nondoped deep-blue organic light emitting devices based on imidazole- $\pi$ -triphenylamine derivatives. *Chem. Mater.* **2012**, *24*, 61–70. [[CrossRef](#)]
26. Thangthong, A.; Meunmart, D.; Prachumrak, N.; Jungstittiwong, S.; Keawin, T.; Sudyoasuk, T.; Promarak, V. Bifunctional anthracene derivatives as non-doped blue emitters and hole-transporters for electroluminescent devices. *Chem. Commun.* **2011**, *47*, 7122–7124. [[CrossRef](#)] [[PubMed](#)]
27. Sun, Y.; Duan, L.; Zhang, D.; Qiao, J.; Dong, G.; Wang, L.; Qiu, Y. A pyridine-containing anthracene derivative with high electron and hole mobilities for highly efficient and stable fluorescent organic light-emitting diodes. *Adv. Funct. Mater.* **2011**, *21*, 1881–1886. [[CrossRef](#)]
28. Choi, I.-S.; Kim, S.H.; Ahn, H.-C.; Kim, Y.; Chung, Y. 2-Triphenylsilyl-9,10-di-1-naphthalenylanthracene and its application for blue organic light emitting diodes. *Bull. Korean Chem. Soc.* **2013**, *34*, 2211–2214. [[CrossRef](#)]
29. Lyu, Y.-Y.; Kwak, J.; Kwon, O.; Lee, S.-H.; Kim, D.; Lee, C.; Char, K. Silicon-cored anthracene derivatives as host materials for highly efficient blue organic light-emitting devices. *Adv. Mater.* **2008**, *20*, 2720–2729. [[CrossRef](#)] [[PubMed](#)]
30. Lee, K.H.; Park, J.K.; Seo, J.H.; Park, S.W.; Kim, Y.S.; Kim, Y.K.; Yoon, S.S. Efficient deep-blue and white organic light-emitting diodes based on triphenylsilane-substituted anthracene derivatives. *J. Mater. Chem.* **2011**, *21*, 13640–13648. [[CrossRef](#)]
31. Kim, R.; Lee, S.; Kim, K.-H.; Lee, Y.-J.; Kwon, S.-K.; Kim, J.-J.; Kim, Y.-H. Extremely deep blue and highly efficient non-doped organic light emitting diodes using an asymmetric anthracene derivative with a xylene unit. *Chem. Commun.* **2013**, *49*, 4664–4666. [[CrossRef](#)] [[PubMed](#)]
32. Wee, K.-R.; Han, W.-S.; Kim, J.-E.; Kim, A.-L.; Kwon, S.; Kang, S.O. Asymmetric anthracene-based blue host materials: Synthesis and electroluminescence properties of 9-(2-naphthyl)-10-arylanthracenes. *J. Mater. Chem.* **2011**, *21*, 1115–1123. [[CrossRef](#)]
33. Choi, I.-S.; Jeong, M.-H.; Lee, S.H.; Park, M.H.; Chung, Y. Synthesis of asymmetric anthracene derivatives and their application for blue organic light-emitting diodes. *Bull. Korean Chem. Soc.* **2016**, *37*, 136–141. [[CrossRef](#)]
34. Wu, C.-H.; Chien, C.-H.; Hsu, F.-M.; Shih, P.-I.; Shu, C.-F. Efficient non-doped blue-light-emitting diodes incorporating an anthracene derivative end-capped with fluorene groups. *J. Mater. Chem.* **2009**, *19*, 1464–1470. [[CrossRef](#)]
35. Chang, Y.-C.; Yeh, S.-C.; Chen, Y.-H.; Chen, C.-T.; Lee, R.-H.; Jeng, R.-J. New carbazole-substituted anthracene derivatives based non-doped blue light-emitting devices with high brightness and efficiency. *Dyes Pigments* **2013**, *99*, 577–587. [[CrossRef](#)]
36. Chen, Y.-H.; Lin, S.-L.; Chang, Y.-C.; Chen, Y.-C.; Lin, J.-T.; Lee, R.-H.; Kuo, W.-J.; Jeng, R.-J. Efficient non-doped blue light emitting diodes based on novel carbazole-substituted anthracene derivatives. *Org. Electron.* **2012**, *13*, 43–52. [[CrossRef](#)]
37. Wu, C.-L.; Chang, C.-H.; Chang, Y.-T.; Chen, C.-T.; Chen, C.-T.; Su, C.-J. High efficiency non-dopant blue organic light-emitting diodes based on anthracene-based fluorophores with molecular design of charge transport and red-shifted emission proof. *J. Mater. Chem. C* **2014**, *2*, 7188–7200. [[CrossRef](#)]

38. Jo, W.J.; Kim, K.-H.; No, H.C.; Shin, D.-Y.; Oh, S.-J.; Son, J.-H.; Kim, Y.-H.; Cho, Y.-K.; Zhao, Q.-H.; Lee, K.-H.; et al. High efficient organic light emitting diodes using new 9,10-diphenylanthracene derivatives containing bulky substituents on 2,6-position. *Synth. Met.* **2009**, *159*, 1359–1364. [[CrossRef](#)]
39. Romain, M.; Tondelier, D.; Geffroy, B.; Jeannin, O.; Jacques, E.; Rault-Berthelot, J.; Poriel, C. Donor/acceptor dihydroindeno[1,2-a]fluorene and dihydroindeno[2,1-b]fluorene: Towards new families of organic semiconductors. *Chem. Eur. J.* **2015**, *21*, 9426–9439. [[CrossRef](#)] [[PubMed](#)]
40. Gao, F.; Ren, J.; Li, Z.; Yuan, S.; Wu, Z.; Cui, Y.; Jia, H.; Wang, H.; Shi, F.; Hao, Y. Trifluoromethyl-substituted 9,9'-bianthracene derivative as host material for highly efficient blue OLED. *Opt. Mater. Express* **2015**, *5*, 2468–2477. [[CrossRef](#)]
41. Yu, Y.; Wu, Z.; Li, Z.; Jiao, B.; Li, L.; Ma, L.; Wang, D.; Zhou, G.; Hou, X. Highly efficient deep-blue organic electroluminescent devices ( $CIE_y \approx 0.08$ ) doped with fluorinated 9,9'-bianthracene derivatives (fluorophores). *J. Mater. Chem. C* **2013**, *1*, 8117–8127. [[CrossRef](#)]
42. Armarego, W.L.F.; Chai, C.L.L. *Purification of Laboratory Chemicals*, 6th ed.; Elsevier: Waltham, MA, USA, 2009; pp. 61–79.
43. Shin, M.-G.; Kim, S.O.; Park, H.Y.; Park, S.J.; Yu, H.S.; Kim, Y.-H.; Kwon, S.-K. Synthesis and characterization of ortho-twisted asymmetric anthracene derivatives for blue organic light emitting diodes (OLEDs). *Dyes Pigments* **2012**, *92*, 1075–1082. [[CrossRef](#)]
44. Park, J.-W.; Kang, P.; Park, H.; Oh, H.-Y.; Yang, J.-H.; Kim, Y.-H.; Kwon, S.-K. Synthesis and properties of blue-light-emitting anthracene derivative with diphenylamino-fluorene. *Dyes Pigments* **2010**, *85*, 93–98. [[CrossRef](#)]



© 2017 by the authors. Licensee MDPI, Basel, Switzerland. This article is an open access article distributed under the terms and conditions of the Creative Commons Attribution (CC BY) license (<http://creativecommons.org/licenses/by/4.0/>).